Molecular Crystals and Liquid Crystals Science and Technology. Section A. Molecular Crystals and Liquid Crystals

Publication details, including instructions for authors and subscription information:
http://www.tandfonline.com/loi/gmcl19

Cation Mixing During Lithium Intercalation into and Deintercalation from $LiAl_yNi_{1-y}O_2$ ($0 \leq y \leq 0.25$) Electrodes

Su-Il Pyun [a], Min-Hyung Lee [a], Heon-Cheol Shin [a] & Sung-Woo Kim [a]

[a] Department of Materials Science and Engineering, Korea Advanced Instituted of Science and Technology, 373-1 Kusong-Dong, Yusong-Gu, Taejon, 305-701, KOREA

Version of record first published: 27 Oct 2006

To cite this article: Su-Il Pyun, Min-Hyung Lee, Heon-Cheol Shin & Sung-Woo Kim (2000): Cation Mixing During Lithium Intercalation into and Deintercalation from $LiAl_yNi_{1-y}O_2$ ($0 \leq y \leq 0.25$) Electrodes, Molecular Crystals and Liquid Crystals Science and Technology. Section A. Molecular Crystals and Liquid Crystals, 341:2, 163-170

To link to this article: http://dx.doi.org/10.1080/10587250008026134

Mol. Cryst. and Liq. Cryst., 2000, Vol. 341, pp. 163-170
Reprints available directly from the publisher
Photocopying permitted by license only

Cation Mixing During Lithium Intercalation into and Deintercalation from $LiAl_yNi_{1-y}O_2$ ($0 \leq y \leq 0.25$) Electrodes

SU-IL PYUN, MIN-HYUNG LEE, HEON-CHEOL SHIN
and SUNG-WOO KIM

Department of Materials Science and Engineering, Korea Advanced Instituted of Science and Technology, 373–1 Kusong-Dong, Yusong-Gu, Taejon 305–701, KOREA

(In final form July 7, 1999)

Cation mixing during lithium intercalation into and deintercalation from $Li_{1-\delta}Al_yNi_{1-y}O_2$ (y = 0; 0.05; 0.25) electrodes was investigated by using galvanostatic intermittent titration technique (GITT) and X-ray diffractometry (XRD). From the XRD patterns obtained from the $Li_{1-\delta}NiO_2$ electrode, the interlayer spacings of the lithium-poorest H3 phase were determined to be smaller than the neighbouring hexagonal H2 phase by 0.03 nm. The cation mixing, i.e., the substitution of nickel ions for lithium vacant sites can account for this shrinkage. The diffusion of lithium ions in the H3 phase was strongly impeded by both the shrinkage of interlayer spacings and the presence of nickel ions in the lithium vacant sites. From the experimental findings that the width of potential plateau at 4.20 $V_{Li/Li+}$ became narrower with increasing aluminum content, y, it was suggested that the substitutive aluminum ions stabilize the layered structure, thus suppressing the cation mixing.

Keywords: cation mixing; $Li_{1-\delta}Al_yNi_{1-y}O_2$ electrodes; galvanostatic intermittent titration technique (GITT); X-ray diffractometry (XRD); aluminum ions

INTRODUCTION

The lithiated transition metal oxides such as $LiCoO_2$[1], $LiNiO_2$[2], and $LiMn_2O_4$[3] have been of great interest as cathode materials for secondary lithium batteries. In particular, $LiNiO_2$ has attracted considerable attention[4,5] because of its low cost and good charge retention compared with the first commercial material $LiCoO_2$. However, the ideal stoichiometric $LiNiO_2$ is difficult to synthesize, and the capacity loss occurs during the overcharge process above 4.20 $V_{Li/Li+}$[6]. Recently, several studies have been devoted to the

stabilization of the layered structure by substituting aluminum ions for nickel ions, i.e., formation of a solid solution with $LiAl_yNi_{1-y}O_2$ ($0 < y \leq 0.25$) composition[7, 8].

This work discusses the cation mixing during the lithium intercalation into and deintercalation from the $Li_{1-\delta}Al_yNi_{1-y}O_2$ (y = 0; 0.05; 0.25) electrodes in terms of measured interlayer spacings and diffusivities of lithium ions in the electrodes. For this purpose, we employed galvanostatic intermittent titration technique (GITT) and X-ray diffractometry (XRD).

EXPERIMENTAL

The $LiAl_yNi_{1-y}O_2$ (y = 0; 0.05; 0.25) powders were prepared by the calcination of pressed mixtures of $LiNO_3$, $Al(OH)_3$, and $NiCO_3$ in a molar ratio of cations at 600 ℃ for 5 h in air, followed by heating them at 750 ℃ for 10 h under an oxygen stream (500 sccm (standard cc per minute)) with intermittent grindings. The prepared oxide powders were then mixed with 6 wt.% Vulcan XC-72 carbon black and 2 wt.% PVDF (poly-vinyliedene fluoride) in NMP (n-methyl pyrrolidone) solution. The stirred mixture was spread on 316 stainless steel ex-met. Upon the evaporation of NMP, the carbon-dispersed composite electrode specimens were dried under vacuum over 6 h.

A three-electrode electrochemical cell was employed for the electrochemical experiments. Both the reference and the counter electrodes were constructed from lithium foil (Foote Mineral Co. U.S.A., purity 99.9%) and 1 M lithium perchlorate ($LiClO_4$) propylene carbonate (PC) solution was used as the electrolyte. The apparent geometric area of the working electrode was 2 cm^2. All electrochemical experiments were conducted at room temperature in a glove box (MECAPLEX GB94) filled with purified argon gas.

Galvanostatic intermittent charge-discharge curve was obtained by using a solartron 1287 Electrochemical Interface (ECI). Applying a constant current to the cell upon charging*, the resulting cell potential transients were recorded. After interruption of the current pulse, the decay of the open circuit potential was followed with time until the fluctuation of the open circuit potential fell below 0.01 V_{Li/Li^+}. This potential value was just recorded as an electrode potential. The application and interruption of the constant current continued until the electrode potential of the $LiNiO_2$ and $LiAl_yNi_{1-y}O_2$ (y = 0.05; 0.25) electrodes reached 4.8 and 4.4 V_{Li/Li^+}, respectively, after which we performed the measurement in the reverse direction, i.e., upon discharging** until the cell potential attained 3.0 V_{Li/Li^+}. In order to characterize the change of crystal

---

* Upon charging the cell by application of anodic current, the lithium deintercalation occurs from the $LiAl_yNi_{1-y}O_2$ electrode.

** Upon discharging the cell by application of cathodic current, the lithium intercalation occurs into the $LiAl_yNi_{1-y}O_2$ electrode.

structures during the lithium intercalation into and deintercalation from the $Li_{1-\delta}NiO_2$ electrode, XRD patterns were recorded at various lithium contents, $(1-\delta)$, on an automated Rigaku powder diffractometer using Cu K_α radiation. The XRD was carried out over the scanning angle 2θ range of 10 ° to 80 ° at the scan rate of 4 °/min.

RESULTS AND DISCUSSION

Figure 1 shows the XRD patterns of the $Li_{1-\delta}NiO_2$ electrode during the lithium deintercalation at various lithium content, $(1-\delta)$. As can be seen in Figs. 1(a), 1(b), and 1(c), it was observed that the hexagonal phase of an as-prepared $LiNiO_2$ electrode, H1, is changed first to monoclinic phase, M, which is further transformed to another hexagonal phases having different lattice parameters, H2 and H3, as lithium is deintercalated.

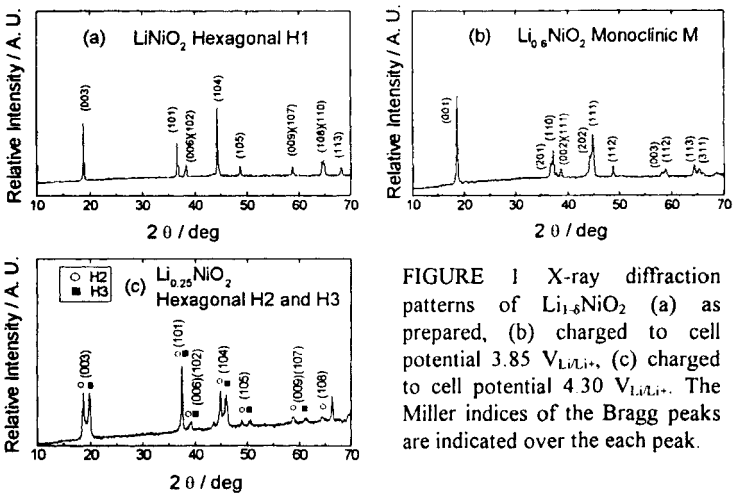

FIGURE 1 X-ray diffraction patterns of $Li_{1-\delta}NiO_2$ (a) as prepared, (b) charged to cell potential 3.85 $V_{Li/Li+}$, (c) charged to cell potential 4.30 $V_{Li/Li+}$. The Miller indices of the Bragg peaks are indicated over the each peak.

The interlayer spacings of the H3 phase were calculated from the analysis of the XRD patterns to be smaller by 0.03 nm in value than those of the H1, M, and H2 phases which are approximately the same. This shrinkage was in good agreement in value with those obtained by Ohzuku et al.[9] and Arai et al.[10] Delmas[11] reported that the considerable shrinkage in H3 phase is strongly caused by the migration of nickel ions into lithium vacant sites. For higher degrees of deintercalation, the layered structure of $Li_{1-\delta}NiO_2$ becomes unstable since the number of remaining Li^+ ions is not large enough to screen the O^{2-}-O^{2-}

repulsions between the two sides of the Van der Waals gap. To stabilize the structure during the overcharge process, some nickel ions move from the slab to the intersheet space. Using Rietveld refinement method, Hirano et al.[12] also found that the nickel ions substituted for lithium ions prevent the lattice distortion during the lithium deintercalation.

Figure 2 demonstrates the first galvanostatic intermittent charge-discharge curve and open circuit potential transients in the potential range of 3.0 V_{Li/Li^+} to 4.8 V_{Li/Li^+} obtained from the Al-undoped $Li_{1-\delta}NiO_2$ electrode as a function of lithium content, (1-δ), in 1 M $LiClO_4$-PC solution. The deviation from the ideal stoichiometry of $LiNiO_2$, δ, was calculated from the values of the mass of the oxide and of the electrical charge that is transferred during the application of current pulses. The open circuit potential transients of the $Li_{1-\delta}NiO_2$ electrode display three potential plateaux at 3.65 V_{Li/Li^+}, 4.00 V_{Li/Li^+}, and 4.20 V_{Li/Li^+}, which proved to be caused by coexistence of H1 and M in equilibrium, M and H2, and H2 and H3, respectively[13].

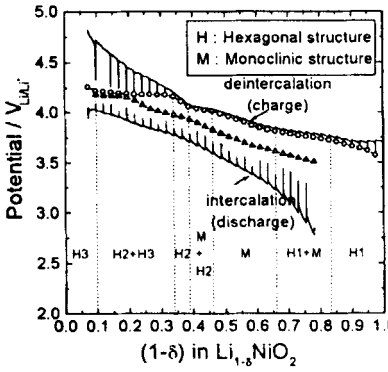

FIGURE 2 First galvanostatic intermittent charge-discharge curve and open circuit potential transients in the potential range of 3.0 to 4.8 V_{Li/Li^+} obtained from the $Li_{1-\delta}NiO_2$ electrode. Open circle and open triangle symbols represent open circuit potentials during charging the cell (deintercalation from the electrode) and discharging the cell (intercalation into the electrode), respectively.

Figures 3(a) and 3(b) illustrate the first galvanostatic intermittent charge-discharge curves in the potential range of 3.0 V_{Li/Li^+} to 4.4 V_{Li/Li^+} obtained from the Al-doped $Li_{1-\delta}Al_{0.05}Ni_{0.95}O_2$ and $Li_{1-\delta}Al_{0.25}Ni_{0.75}O_2$ electrodes, respectively, as a function of lithium content (1-δ) in 1 M $LiClO_4$-PC solution. From the comparison of the first galvanostatic charge-discharge curves for the Al-doped $Li_{1-\delta}Al_yNi_{1-y}O_2$ (y = 0.05; 0.25) electrodes with those results for the Al-undoped $Li_{1-\delta}NiO_2$ electrode, it was found that the potential plateau at 4.20 V_{Li/Li^+} was narrowed in width with aluminum content and finally the potential plateau disappeared in the Al-doped $Li_{1-\delta}Al_{0.25}Ni_{0.75}O_2$ electrode. This means that the layered structure of the $Li_{1-\delta}Al_yNi_{1-y}O_2$ electrodes is stabilized by the substitutive aluminum ions. As a consequence, the cation mixing is suppressed during the lithium deintercalation with aluminum content and finally it does not occur in the Al-doped $Li_{1-\delta}Al_{0.25}Ni_{0.75}O_2$ electrode. Such an impediment of the cation

mixing with aluminum content improves the reversibility between the lithium intercalation into and deintercalation from the electrodes with charge-discharge cycle[14].

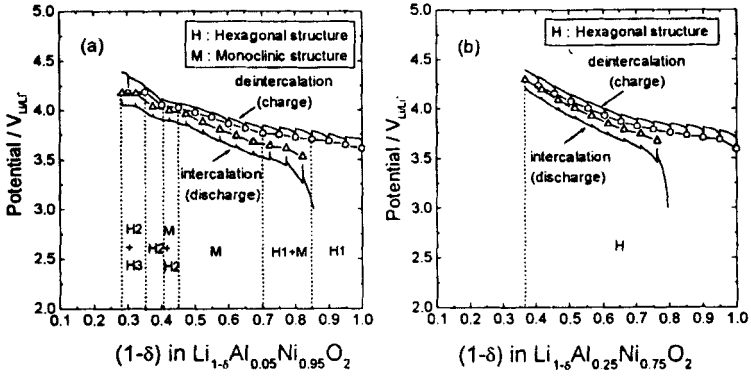

FIGURE 3 First galvanostatic intermittent charge-discharge curve and open circuit potential transients in the potential range of 3.0 to 4.4 V_{Li/Li^+} obtained from the (a) $Li_{1-\delta}Al_{0.05}Ni_{0.95}O_2$ and (b) $Li_{1-\delta}Al_{0.25}Ni_{0.75}O_2$ electrodes. Open circle and open triangle symbols represent open circuit potentials during charging the cell (deintercalation from the electrode) and discharging the cell (intercalation into the electrode), respectively.

The chemical diffusivities of lithium ions in the $Li_{1-\delta}Al_yNi_{1-y}O_2$ electrodes at various lithium content were calculated by using Eq. (1) from galvanostatic intermittent charge-discharge curves[15] :

$$\tilde{D}_{Li^+,\,chem} = \frac{4}{\pi}\left(\frac{V_m}{SF}\right)^2\left[I_0\left(\frac{dE}{d\delta}\right)\Big/\left(\frac{dE}{d\sqrt{t}}\right)\right]^2 \qquad (1),$$

where $\tilde{D}_{Li^+,\,chem}$ is the chemical diffusivity of lithium ions (cm^2s^{-1}); V_m, the molar volume ($cm^3\,mol^{-1}$); S, the geometric apparent area of the electrode/electrolyte interface (cm^2); F, the Faraday constant; I_0, the applied constant current (A); $dE/d\delta$, the slope of the coulometric titration curve and $dE/d\sqrt{t}$ represents the slope of the E versus square root of time curve.

Considering thermodynamic enhancement factor obtained from the coulometric titration curve, the component diffusivities of lithium ions in the electrodes were calculated from Eq. (2)[15] :

$$D_{Li^+,comp} = -\frac{RT}{(1-\delta)F}\left(\frac{d\delta}{dE}\right)\tilde{D}_{Li^+,chem} \quad (2),$$

where $D_{Li+,comp}$ is the component diffusivity of lithium ions (cm^2s^{-1}); R, the gas constant; T, the absolute temperature and $-[RT/(1-\delta)F](d\delta/dE)$ represents the inverse of the thermodynamic enhancement factor. The component diffusivity is a measure of the random motion of lithium ions in the absence of a concentration gradient and is mainly determined by the number of vacant sites available for the jump of lithium ions in the oxide and the structural modification of the oxide induced by the intercalated lithium ions[16, 17].

The chemical and the component diffusivities of lithium ions in the single phases such as H1, M, H2, and H3 during the lithium deintercalation from the $Li_{1-\delta}Al_yNi_{1-y}O_2$ (y = 0; 0.05; 0.25) electrodes are plotted in Figs. 4(a) and 4(b), respectively, as a function of lithium content, (1-δ). The diffusivities of lithium ions obtained from the $Li_{1-\delta}Al_yNi_{1-y}O_2$ (y = 0; 0.05; 0.25) electrodes in the range of (1-δ) ≥ 0.4 decreased with lithium content. The decrease in the diffusivities with lithium content is attributable to the reduced number of vacant sites available for the jump of lithium ions[16, 17].

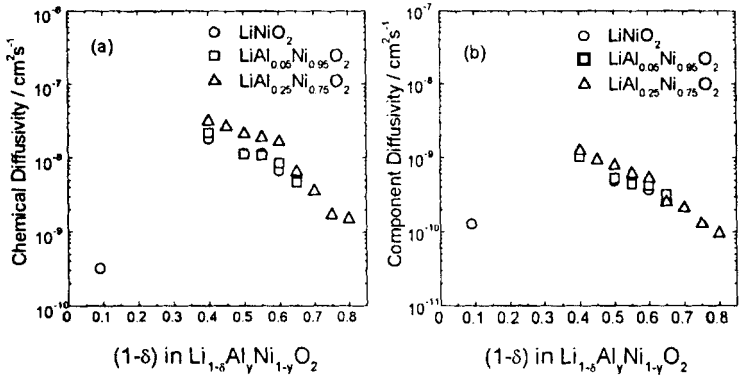

FIGURE 4 (a) Chemical diffusivity, $\tilde{D}_{Li^+,chem}$, and (b) component diffusivity, $D_{Li^+,comp}$, of lithium ions in the $Li_{1-\delta}Al_yNi_{1-y}O_2$ (y = 0; 0.05; 0.25) electrodes during the lithium deintercalation as a function of lithium content (1-δ) at room temperature.

In the case of the Al-undoped $Li_{1-\delta}NiO_2$ electrode, the diffusivities of lithium ions in the H3 phase in the range of (1-δ) ≤ 0.1, were smaller in value than those in the H2 and M phases by about one or two orders of magnitude. This suggests that the diffusion of lithium ions through the H3 phase is strongly

impeded by the shrinkage of interlayer spacings and the presence of nickel ions in the lithium vacant sites. On the other hand, the diffusivities in the Al-undoped $Li_{1-\delta}NiO_2$ electrode at various lithium contents above $(1-\delta) = 0.4$ were nearly the same in value with those of the Al-doped $Li_{1-\delta}Al_yNi_{1-y}O_2$ ($y = 0.05$; 0.25) electrodes. It is indicated that the cation mixing impeding the diffusion of lithium ions does not occur in this range of $(1-\delta) \geq 0.4$.

CONCLUSIONS

In the present work, the cation mixing during lithium intercalation into and deintercalation from the $Li_{1-\delta}Al_yNi_{1-y}O_2$ ($y = 0$; 0.05; 0.25) electrodes has been discussed in view of interlayer spacings and diffusivities of lithium ions determined from XRD patterns and galvanostatic intermittent charge-discharge curves, respectively. The results are summarized as follows;

1. The diffusivities of lithium ions in the H3 phase of the Al-undoped $Li_{1-\delta}NiO_2$ electrode were smaller in value than those in other phases such as the monoclinic M and hexagonal H2 phases by about one or two orders of magnitude. This suggests that the diffusion of lithium ions within the H3 phase is strongly impeded by both the shrinkage of interlayer spacings and the presence of nickel ions in the lithium vacant sites as confirmed from the analysis of the XRD patterns.
2. As aluminum content y in the Al-doped $Li_{1-\delta}Al_yNi_{1-y}O_2$ electrodes increased, the potential plateau at 4.20 V_{Li/Li^+} which results due to the coexistence of H2 and H3 phases was more narrowed in width. This means that the aluminum ions stabilize the layered structure, thus impeding the cation mixing.

Acknowledgements

The authors are grateful to the Ministry of Commerce and Industry, Korea 1998/1999 and in part the KOSEF 1998/1999 through the CISEM at KAIST for financial support of this work.

References

[1] K. Mizushima, P. C. Jones, P. J. Wiseman, and J. B. Goodenough, *Mater. Res. Bull.* **15,** 783 (1980).
[2] J. Morales, C. Perez-Vicente, and J.L. Tirado, *Mat. Res. Bull.* **25,** 623 (1990).
[3] M. M. Thackeray, P. J. Johnson, L. A. de Picciotto, P. G. Bruce and J. B. Goodenough, *Mat. Res. Bull.* **19,** 179 (1984).
[4] J.R. Dahn, U. von Sacken, and C.A. Michal, *Solid State Ionics* **44,** 87 (1990).
[5] M. Broussely, F. Perton, P. Biensan, J. M. Bodet, J. Labat, A. Lecerf, C. Delmas, A. Rougier, and J. P. Peres, *J. Power Sources* **54,** 109 (1995).
[6] H. Arai, S. Okada, Y. Sakurai, and J. Yamaki, *Solid State Ionics* **95,** 275 (1997).
[7] T. Ohzuku, A. Ueda, and M. Kouguchi, *J. Electrochem, Soc.* **142,** 4033 (1995).
[8] Q. Zhong and U. von Sacken, *J. Power Sources* **54,** 221 (1995).
[9] T. Ohzuku, A. Ueda, and M. Nagayama, *J. Power Sources* **140,** 1862 (1993).
[10] H. Arai, S. Okada, H. Ohtsuka, M. Ichimura, and J. Yamaki, *Solid State Ionics* **80,** 261 (1995).

[11] C. Delmas, *Mat. Sci. & Eng.* **B3,** 97 (1989).
[12] A. Hirano, R. Kanno, Y. Kawamoto, Y. Takeda, K. Yamada, and M. Takano, *Solid State Ionics* **78,** 123 (1995).
[13] W. Li, J. N. Reimers, and J. R. Dahn, *Solid State Ionics* **67,** 123 (1993).
[14] M.-H. Lee, Korea Advanced Institute of Science and Technology, M.S. Thesis (in English) (1999).
[15] W. Weppner and R. A. Huggins, *J. Electrochem. Soc.* **124,** 1569 (1977).
[16] Y.-M. Choi, S.-I. Pyun, J.-S. Bae, and S.-I. Moon, *J. Power Sources* **56,** 25 (1995).
[17] Y.-M. Choi, S.-I. Pyun, and S.-I. Moon, *Solid State Ionics* **89,** 43 (1996).